Rational and affordable concepts of Landing Gear for small reentry vehicle demonstrators

Rational and affordable concepts of Landing Gear for small reentry vehicle demonstrators

S. Chiesa[1], D. Cardile[2], M. Fioriti[3], and N. Viola[4]
Politecnico di Torino, Turin, Italy, 10129

The paper proposes an innovative solution for landing gear of small space vehicles, in particular of technological demonstrators of reentry space vehicles. After explaining why small space vehicles can benefit from landing gears, the work investigates a solution, which avoids the use of fluidic systems and minimizes constraints on the whole vehicle, thus limiting cost raising and making the installation of the landing gear easier on vehicles that originally did not envisage landing gears.

Nomenclature

b	=	Length of the leaf spring side perpendicular to the deflection plane
b_E	=	Length of the side perpendicular to the deflection plane at the free end of the leaf spring
b_R	=	Length of the side perpendicular to the deflection plane at the root of the leaf spring
CoG	=	Center of Gravity
E	=	Elastic modulus
f	=	Deflection
$F_{braking}$	=	Braking Force
FAR	=	Federal Aviation Regulation
g	=	Acceleration of gravity
GNC	=	Guidance Navigation and Control
h	=	Leaf spring thickness
H	=	Distance from Center of Gravity to the Runway
I	=	Moment of inertia
K_2	=	Section ratio
K_b	=	Non linearity effects coefficient
K_{fl}	=	Lateral friction coefficient of the tire
K_l	=	Landing load factor
l	=	Length of the leaf spring
L	=	Lift
L_{wb}	=	Wheel Base
LDG	=	Landing Gear
M	=	Bending moment
$MLDG$	=	Main Landing Gear
n_M	=	Distance from Main Gear to the Center of Gravity
n_N	=	Distance from Nose Gear to the Center of Gravity
N	=	Landing gear load factor
$NASA$	=	National Aeronautics and Space Administration
$NLDG$	=	Nose Landing Gear
R_{MLDG}	=	Force on Main Landing Gear
R_{NLDG}	=	Force on Nose Landing Gear
RRV	=	Reference Re-entry Vehicle
S	=	Leaf spring vertical displacement
S_0	=	Leaf spring horizontal displacement

[1] Full Professor, Department of Mechanical and Aerospace Engineering, sergio.chiesa@polito.it.
[2] PhD Student, Department of Mechanical and Aerospace Engineering, diego.cardile@polito.it.
[3] Researcher, Department of Mechanical and Aerospace Engineering, marco.fioriti@polito.it.
[4] Assistant Professor, Department of Mechanical and Aerospace Engineering, nicole.viola@polito.it.

S_w = Compression of the tire
T_f = Taper Factor
TRL = Technology Readiness Level
UAV = Unmanned Aerial Vehicle
US = United States
V_z = Vertical speed
W = Maximum landing weight of the vehicle in static condition
ζ = Landing gear's maximum acceptable percentage of height lost during compression
θ = Angle between the leaf spring and the horizontal direction
σ_{amm} = Yield stress
$\ddot{X}$ = Acceleration

I.Introduction

WITHIN the vast framework of activities for the development of future reliable trans-atmospheric transport vehicles, nowadays great efforts are directed towards technological demonstrators of the same vehicles on a reduced scale[1,2]. Many of these technological demonstrators aim at developing, testing and validating quite a few technologies that have not reached yet the necessary TRL level. In this context we believe that a dramatic improvement could be represented by the use of landing gears, in order to make the technological demonstrator land like an airplane on the runway, thus verifying this fundamental capability for future space vehicles and studying more into details all issues related to GNC. With the aim of making the development, test and validation of innovative applications of landing gears easier, the paper presents a concept of a particularly simple landing gear for small technological demonstrators of reentry vehicles.

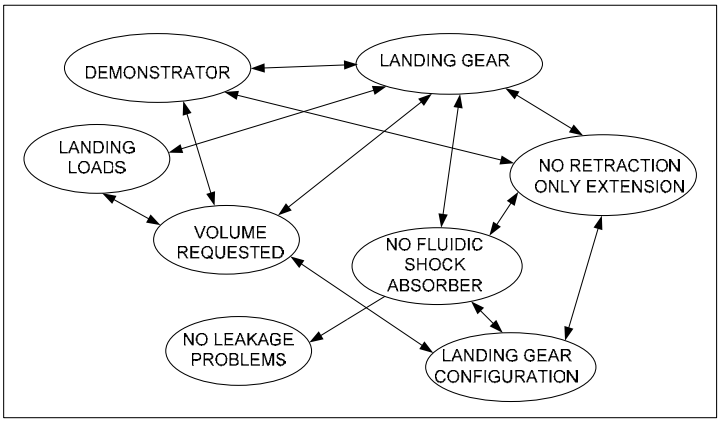

Figure 1. Small reentry vehicle landing gear influences and constraints

As the relationship diagram depicted in Fig. 1 shows, the landing gear has to be integrated with the technological demonstrator and correctly sized to bear landing loads, by elastically absorbing the vertical kinetic energy of the vehicle at touchdown and by dissipating it. As far as the integration of the landing gear with the vehicle is concerned, two issues deserve particular attention: the cavity inside the vehicle to stow the retracted landing gear and the structural discontinuities to let the landing gear be extracted. The concept of landing gear presented in the paper is characterized more by the capability of adapting to the vehicle's structural configuration rather than by the necessity of constraining it. If we think of costs, there are two considerations that may enhance affordability of landing gears of small technological demonstrators: as small technological demonstrators do not generally take-off autonomously (being transported to orbit by launcher vehicles), the landing gear does not have to be retracted, whereas its extension during approach and landing occurs thanks mainly to gravity, therefore avoiding the use of dedicated actuators; the use of fluidic shock absorbers could be avoided as well. Taking these considerations into account, a good solution for the landing gear of small technological demonstrators of re-entry vehicles appears to be the leaf spring landing gear[3], typical of light aircraft, where dissipation of aircraft vertical kinetic energy is given by the tires' side scrubbing[4], caused by the leaf spring deflection. An alternative solution could be the rubber disk or steel spring shock absorber which are able to dissipate the touchdown energy by the internal attrition between, respectively, the disks or the spring rings. If fluidic shock absorbers and generally fluidic systems shall be avoided, the use of electric brakes acting on the wheels of the main landing gear appears to be quite obvious. The differential activation of these brakes allows turning the small vehicle on ground. Therefore, as the specific capability of on ground maneuvering shall not be required for this type of vehicle, the steering function of the nose landing gear shall not be implemented.

Eventually we can say that the design of the landing gear seems to be driven mainly by those elements that have to perform the functions of absorbing and damping landing loads. These elements shall seriously affect both the configuration and the sizing of the landing gear and, consequently, the sizing of the cavity inside the vehicle, where the landing gear has to be stowed when retracted.

II. General landing gear configuration

As it is well known, the landing gear arrangement consists of at least three struts with at least one wheel each. Landing gear's struts have to be at least three because they have to define an area, within which the vertical projection of the vehicle's center of gravity (CoG) has to fall with adequate margins, in order to avoid the risk for the vehicle to turn over during taxi, as shown in Fig. 2.

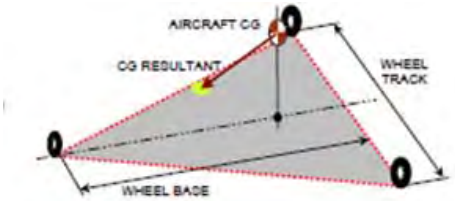

Figure 2. Landing Gear elements location vs

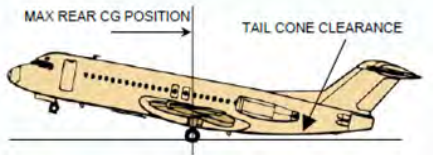

Figure 3. Main LDG elements position and Tail Cone Clearance

Apart from the movement of the vehicle on ground during taxi, during touchdown the landing gear has to be able to absorb the vehicle's vertical kinetic energy, without generating excessively high loads on the vehicle's structure, specifically on the landing gear's joints to the vehicle's structure. During touchdown the vehicle's vertical kinetic energy has to be absorbed but also dissipated by the landing gear, in order to avoid vehicle's bounces (an undesirable phenomenon which in the past led to catastrophic events). As well as during taxi, also during touchdown it is extremely important that the vehicle does not turn over, taking also into account the high value of the vehicle's attitude at touchdown, in order to minimize vehicle's speed. As at touchdown the contact between the vehicle and the ground occurs first through the rear wheels of the landing gear, there is the need for an adequate clearance between the ground and the back of the vehicle (tail cone), as shown in Fig. 3. The fact that the rear wheels (main elements) of the landing gear touch first the ground has led to the following choices:

a) the main elements of the landing gear have to be at least two, in order to guarantee the vehicle's lateral stability not only during taxi but also during touchdown, when the vehicle touches the ground with one of the two main element first, as it is not in level flight;

b) the two main elements are bigger than the third element (Nose Landing Gear), located in a central, fore position, as the main elements are in charge of absorbing most of the vertical kinetic energy at touchdown;

c) the main elements, located behind the vehicle's CoG, have to be as close as possible to the vehicle's CoG for the very same reasons mentioned above but they have however to guarantee that the vertical projection of the vehicle's CoG falls inside the area defined by the landing gear ground contact points in every mission phase, included landing when the vehicle flies at high angle of attack at touchdown (see Fig. 3);

d) taking into account the above mentioned configuration, after the very first touchdown, the vehicle rotates around the axis of the wheels' contact with ground until the Nose Landing Gear touches the ground and the vehicle starts the deceleration phase, in order to dissipate also the horizontal kinetic energy, connected to the horizontal component of the vehicle's speed at touchdown (definitely higher than the vertical kinetic energy at touchdown).

Table 1. Martin Marietta X24A Technical Data

Crew	1
Length	7.47 m
Wingspan	3.51 m
Height	2.92 m
Wing area	18.1 m²
Empty weight	2,885 kg
Loaded weight	4,853 kg
Max. takeoff weight	5,192 kg
Power plant	1xReaction Motor XLR-11rs rocket engine, 37.7 kN
Maximum speed	1,667 km/h
Range	72 km
Service ceiling	21,763 m
Wing loading	288 kg/m²
Thrust/weight	0.70

III. Review of technical solutions for landing gear's reentry space vehicles

The use of landing gears for reentry space vehicles is not a new idea, since a few examples, especially in US, do already exist. However the purpose of the paper is to let the technology of landing gears come closer to other countries and other agencies that, notwithstanding their

work in the space field, have not yet gathered a great deal of experience in landing gears for reentry vehicles.

These examples represent a fundamental base of knowledge, the real starting point to build up new and original solutions for landing gears of reentry space vehicles. Studying and understanding what has already been designed and developed is in fact crucial to elaborate innovative ideas. This section deals therefore with a review of the most significant examples of reentry space vehicles with landing gear. Only small size vehicles have been considered.

The first vehicle of this brief review is Martin Marietta X24A, whose main technical data are listed in Table 1. Figure 4a) shows the three view drawing of Martin Marietta X24A, whereas Fig. 4b) illustrates the internal layout of its subsystems. Martin Marietta X24A was developed at the end of 1960s mainly to study the aerodynamic behavior of lifting body configurations. Its landing weight was a bit less than three tons. It was a manned vehicle with one pilot on-board. The configuration of its landing gear was very similar to those used for aircraft with the retraction of the landing gear rearward along planes parallel to the plane of vehicle's longitudinal symmetry. Thanks to the wide fuselage, the wheel track is good and the retraction is fairly easy without any interference with the wing structure.

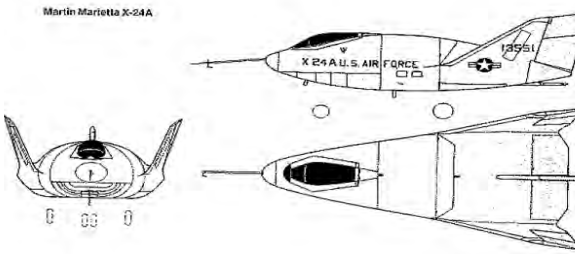

Figure 4a). Martin Marietta X24A

Figure 4b). Martin Marietta X24A internal systems

The second vehicle that we have been taken into consideration is Lockheed X24C, which was a project to fatherly develop Martin Marietta X24A by enhancing its capability of extremely high speed of flight.

Main technical data of Lockheed X24C are reported in Table 2. Figure 5a) shows the three view drawing of Lockheed X24C, whereas Fig. 5b) illustrates the internal layout of its subsystems. The same considerations made for the previous vehicle, still apply to Lockheed X24C, which is very streamlined.

Table 2. Lockheed X24C Technical Data

Length	22.81 m
Wingspan	7.37 m
Wing area	53 m² (estimated)
Height	6.27 m
Crew	1
Gross weight	29934 kg
Empty weight	9691 kg
Max altitude	28042 m
Max speed	7170 km/h

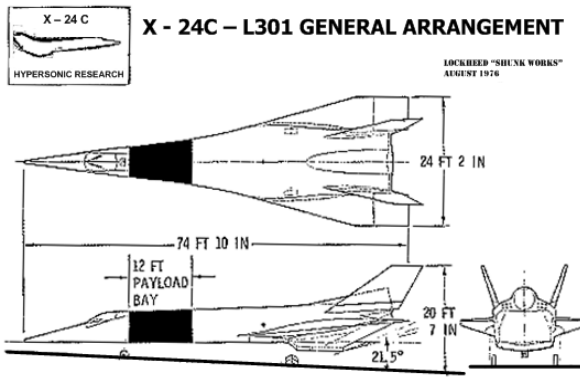

Figure 5a). Lockheed X24C

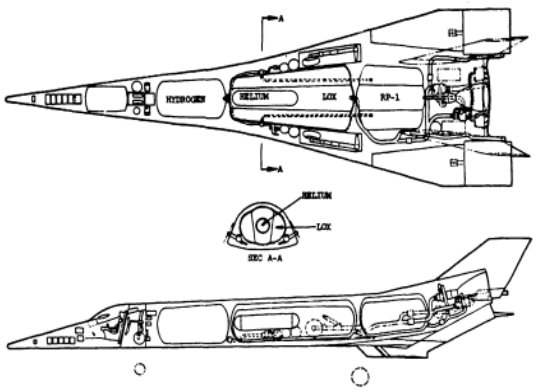

Figure 5b). Lockheed X24C internal arrangement

The third vehicle that we have been taken into consideration is Orbital Sciences X-34, which was designed as technological demonstrator of hypersonic reentry and landing on runways. Orbital Sciences X-34 was really constructed and flew few times but the program was eventually cancelled by NASA in 2001. Main technical data of Orbital Sciences X-34 are reported in Table 3. Figure 6a) shows the three view drawing of Orbital Sciences X-34, whereas Fig. 6b) illustrates the internal layout of its subsystems. Orbital Sciences X -34 was an unmanned vehicle and its landing weight was considerably high, if compared to the landing weights of small technological demonstrators.

Table 3. Orbital Sciences X-34 Technical Data

Length	17.78 m
Wingspan	8.43 m
Wing area	33.21 m²
Height	3.5 m
Gross weight	21319 kg
Empty weight	7711 kg
Range	885 km
Max altitude	76200 m
Max speed	8626 km/h

The landing gear of Orbital Sciences X-34 has a traditional configuration, very similar to landing gears of civil transport aircraft. As Fig. 6b) shows that the main landing gear elements are located behind wing main structure and are retracted sidewise, thus having a simple solution with a very good wheel track.

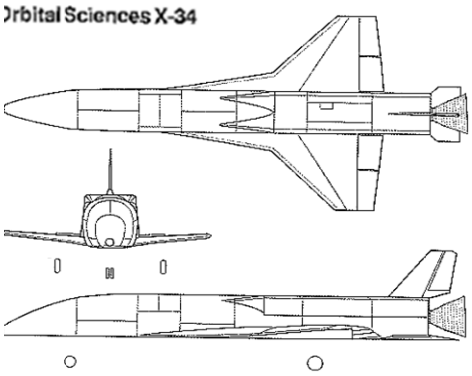

Figure 6a). Orbital Sciences X -34

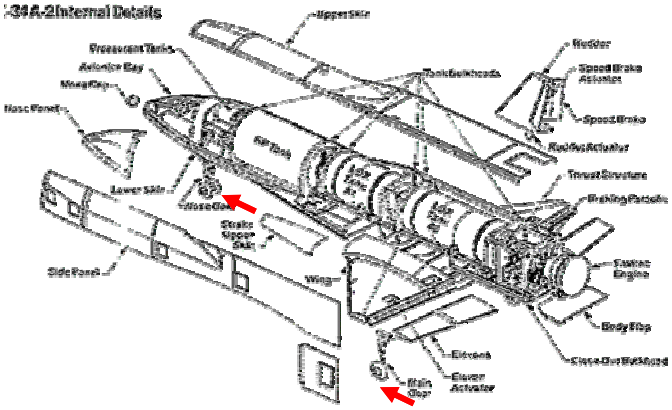

Figure 6b). Orbital Sciences X -34 internal arrangement

Boeing X-37 (see Fig. 7b) and Table 4) and Boeing X-40 (see Fig. 8 and Table 5), which are very close in time, are both unmanned vehicles and have both small size and reduced weight. Their configurations are similar, as Boeing X-40, which is a little bit smaller than Boeing X-37, has been designed as technological demonstrator of Boeing X-37. In particular, Boeing X-40, which is deployed by helicopters, aims at investigating the landing mission phase. Boeing X-37 has been launched twice by ATLAS V launcher vehicle. It has orbited around the Earth and has eventually landed completely autonomously. As Fig. 7b) and Fig. 8 show, the landing gears, which have a traditional configuration, are located on the fuselage side and are retracted through a forward rotation along the longitudinal plane, as the internal arrangement of Boeing X-37 in Fig. 7a) shows for a study of a future manned version.

Table 4. Boeing X–37 technical data

Length	8.38 m
Gross weight	5443 kg
Empty weight	? kg
Wing span	4.57 m
Wing area	7 m²
Mach	25

Table 5. Boeing X – 40 technical data

Length	6.7 m
Length (w/pilot)	6.7 m
Wingspan	3.5 m
Wing area	3.86 m²
Height	2.2 m
Gross weight	1200 kg
Empty weight	? kg
Range	? km
Max altitude	2743 m
Max speed	1609 km/h

Figure 7a). Boeing X-37 Internal arrangement

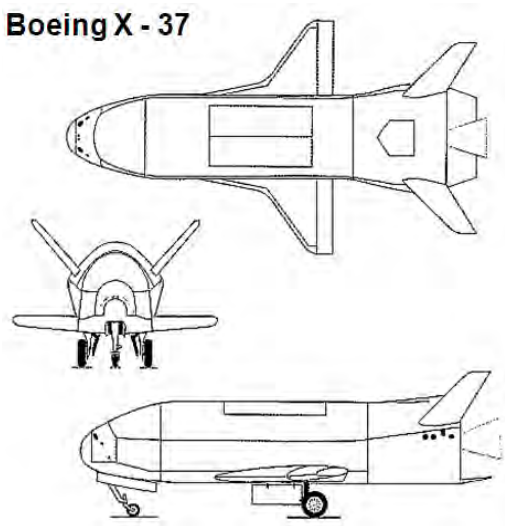

Figure 7b). Boeing X-37

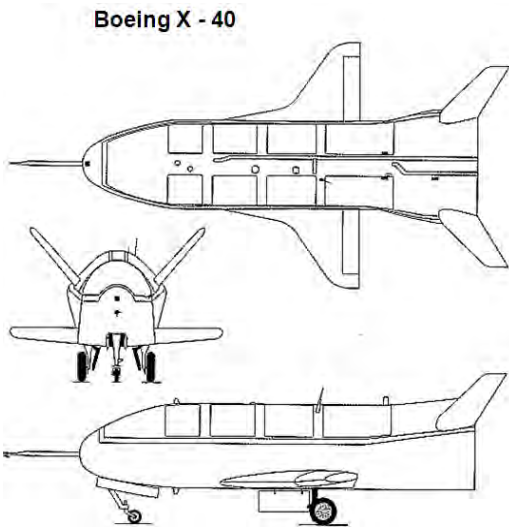

Figure 8. Boeing X-40

As last example of reentry space vehicle equipped with landing gear, Fig. 9 shows the so-called "Dream Chaser", which is the first example of commercial space transport vehicle currently under way. The Dream Chaser may be injected into orbit by ATLAS V launcher vehicle and may carry up to seven people on board. After orbiting around the Earth, it will land on runways autonomously. As reported in Table 6, the weight of Dream Chaser will be not too higher than that of Boeing X-37, whereas its configuration reminds some features of the first Lifting Bodies, like the X-24a (and this is true also for the configuration of the landing gear).

Table 6. NASA Dream Chaser technical data

Length	9 m
Wingspan	7 m
Mass	11340 kg
Crew	Up to 7
Endurance	210 days
Re-entry "g"	<1.5

In brief, on the basis of the analyses of past projects, it is clear that the general configuration, which may be suitable for the landing gear of a technological demonstrator of a future reentry vehicle of small size, should be traditional. However we believe that some innovative solutions should be investigated, in order to pursue the fundamental objectives of reduced cost and reduced impact on the whole vehicle, according to requirements mentioned in section I.

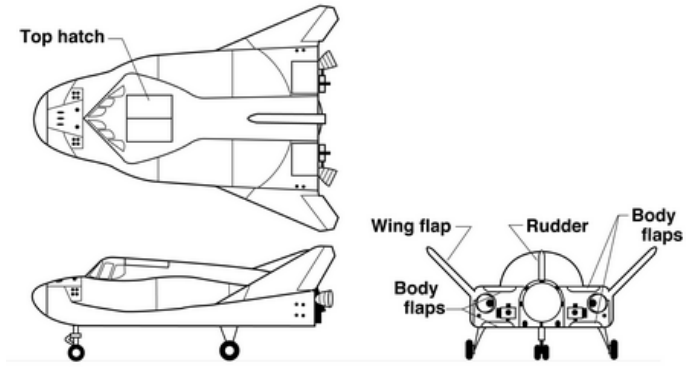

Figure 9. NASA Dream Chaser

IV.A simple solution: the Leaf Spring Landing Gear

A. General overview

The Leaf Spring Landing Gear consists of one elastic element, which is the leg of MLDG elements itself. As shown in Fig. 10, when the wheel touches the ground, the leg deflects elastically and the lateral movement of the tire (toward the outside when the leaf spring is deflected and toward the inside when the spring straightens to the static load position) damps the vertical energy of the whole vehicle at touchdown, thanks to its high lateral friction coefficient.

The elastic element, i.e. the landing gear leg, may be either a box-type beam or a metal leaf, from which the name Leaf Spring derives.

Figure 10. Leaf Spring Landing Gear

B. Examples

The Leaf Spring Landing Gear is very simple and this feature implies low cost and high reliability. These two fundamental characteristics are the reasons of the widespread use of the Leaf Spring Landing Gear in light and ultralight aircraft. Main disadvantages of this type of landing gear are its size and consequently its volume, which makes it not retractable in light and ultralight aircraft, and the rapid wear of the tire, because of the aforesaid lateral displacement. It is worth noting that the latter disadvantage appears to be not so critical for vehicles that are not continuously operative and certainly not so important for reentry space vehicles. However, thinking of reentry space vehicles, the Leaf Spring Landing Gear can be adopted only if retractable into a cavity that has the least effect on basic airframe structure and this goal can be reached simply by considering a linear and not a curved elastic element. Examples of this solution are a few recent Unmanned Aerial Vehicles (UAV), like the well know General Atomics Predator A (illustrated in Fig. 11a) and Fig. 11b)) e General Atomic Predator B (illustrated in Fig. 12a) and Fig. 12b)). Main technical data of these two UAV are summarized in Table 7 and Table 8. Eventually Fig. 13 and Fig. 14 show respectively that the landing gear of Predator A and Predator B is stowed in a very small cavity when retracted.

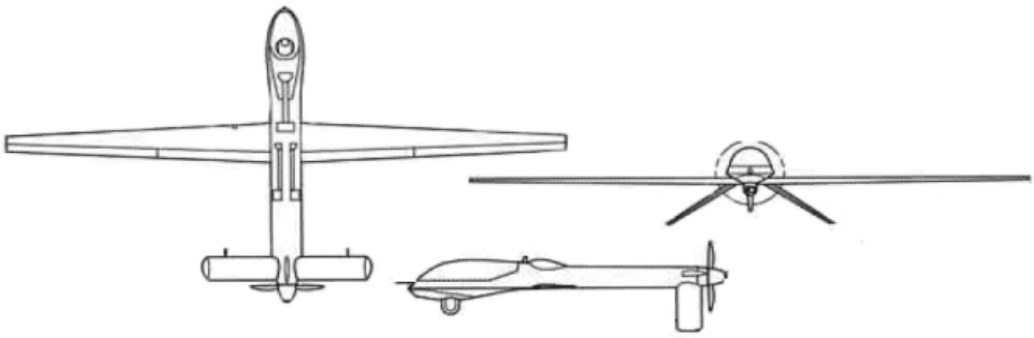

Figure 11a). General Atomics "Predator" A

Figure 11b. General Atomics "Predator" A

Table 7. G.A. "Predator" A technical data

Length	22 m
Wing span	14.8 m
High	1.82 m
Wing area	11.5 m²
Empty weight	512 kg
Max weight	952 kg / 1020 kg
Power plant	Rotax 912 (o 914) 4 cylinders
Power	100 CV / 115 CV
Maximum speed	217 km/h
Range	926 km
Maximum altitude	7800 m

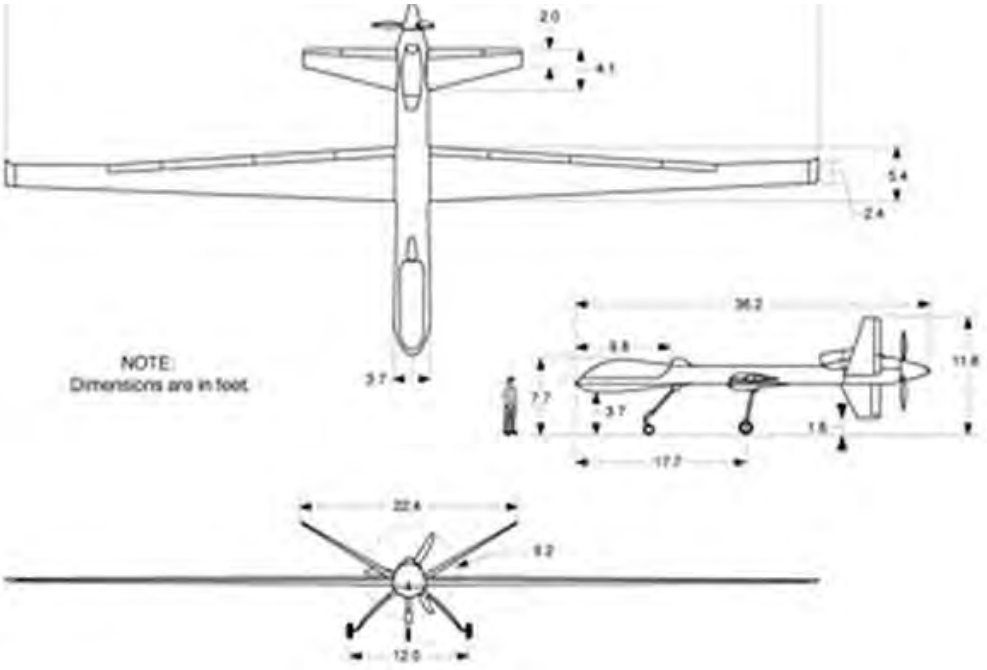

Figure 12a). General Atomics "Predator" B

Figure 12b). General Atomics "Predator" B

Table 8. G.A. "Predator" B technical data

Length	10.97 m
Wingspan	20.12 m
Height	3.56 m
Weight max	4540 kg
Weight empty	1380 kg
Speed	> 405 km/h
Ceiling	15200 m
Endurance	> 24 h
Power plant	Honeywell TPE-331-10T turboprop
Power	670 kW

Figure 13. Predator A landing gear retraction vanes

Figure 14. Predator B landing gear retraction vanes

C. Calculation model

As it usually happens during the design process, once qualitative choices are made, quantitative analyses begin to correctly size and verify the concept, in order to validate and eventually adopt the solution. Quantitative analyses start from the definition of the various requirements that drive the design of the Leaf Spring Landing Gear. Within requirements, initial data, hypotheses and constraints have also to be determined (see Fig. 15 and Fig. 16). For the design of every type of landing gear, one of the most important requirements is the capability of the vehicle of sustaining the loads transmitted by the Main Landing Gear elements at touchdown. As shown in Fig. 15 during landing the Main Landing Gear transmits to the vehicle's structure a load equal to W multiplied by N, where W is the maximum landing weight of the vehicle in static condition and N is the landing gear load factor, expressed as number of g (acceleration of gravity), in order to consider the deceleration of the vehicle along the vertical axis (which in Aeronautics may range between 2,5 for commercial transport aircraft and 9 for fighter aircraft). The extra-load (this load comprises the static load plus the dynamic reaction load) experienced by the vehicle at touchdown is due to vertical speed Vz of the vehicle at touchdown, which is related both to the aeromechanical characteristics of the vehicle itself and to the trajectory chosen for landing. This vertical speed may therefore be constrained by rules of Airworthiness Regulations (see Table 9[5]).

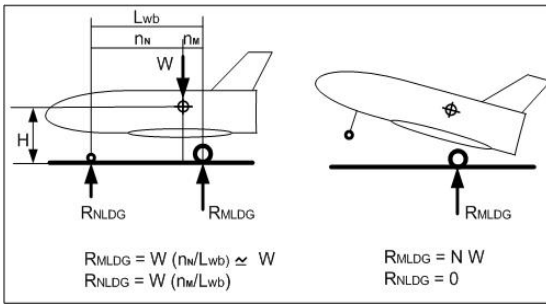

Figure 15. LDG loads (in static conditions and at Landing)

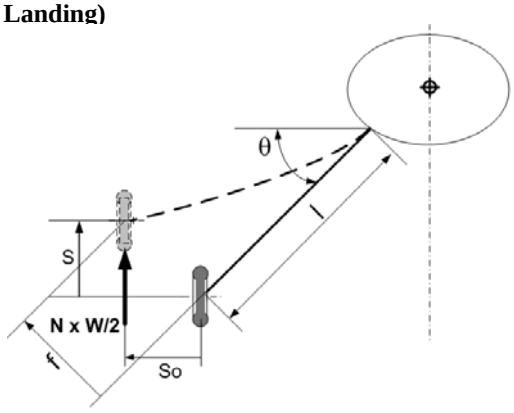

Figure 16. MLDG element, unloaded and at touchdown

Table 9. Vertical Speed at Landing

FAR 23:	$w_t = 4.4(W/S)_L^{1/4}$, but no less than 7 and no more than 10 fps (Derived from FAR 23.725)
FAR 25:	w_t = 12 fps (FAR 25.723)
USAF:	w_t = 10 fps (13 fps for trainers)
USN:	w_t = 10 fps for transports
	w_t = 17 fps for other non-carrier based airplanes

Taking now into account Fig. 16, we can say that the geometry of the Leaf Spring Main Landing Gear is defined by the length of the leaf spring, l, and by the angle, θ, between the leaf spring and the horizontal direction. During flight, i.e. when the Main Landing Gear is unloaded, the angle θ is pretty close to 45°, as the pictures of Predator show. At touchdown the leaf spring is deflected upwards because of the loads applied to the wheel. Immediately after touchdown the vertical component of leaf deflection progressively increases up to a certain value S (see Fig. 16), which corresponds to the maximum load applied to wheel and equal to $\frac{NW}{2}$, in case of symmetric landing on the two main landing gear elements. As shown in Fig. 16, S is the vertical component of deflection, f, of the leaf spring, which is considered as a beam with one end built in and the free end with the load. As first approximation, the relationship between S and f is given by:

$$S = f \cos \theta \tag{1}$$

The horizontal displacement, S_0, of the leaf spring (i.e. the wheel) is given by:

$$S_0 = S \tan\theta \, K_b \tag{2}$$

where the coefficient K_b is slightly less than one to take into account non linearity effects.

The total vertical deflection experienced by the leaf spring is given by the sum of S and S_w, which expresses the compression of the tire, as follows:

$$S_{tot} = f \cos\theta + S_w \tag{3}$$

It is worth noting that S_w has no effect on S_0.

Inputs of the sizing activity of the Leaf Spring Landing Gear are therefore W, l and θ, which come respectively from the vehicle's global characteristics and the landing gear's geometry, and V_z, sink speed at touchdown, N, landing load factor and K_l, the ratio between the mean value of lift, L, during leaf spring compression and weight W. All these three last inputs may be established by Airworthiness Regulations .As far as the sink speed at touchdown, V_z, is concerned, there is no doubt that its value derives from Regulations. As far as the landing load factor, N, is concerned, in order to optimize the whole vehicle, its value may be considered not too far from the maximum values for the load factor required by Regulations (if applicable). Eventually as far as the ratio K_l, which takes into account that during the deflection of the main landing gear elements the vehicle tends to pitch down (because of the forward position of the CoG), thus reducing the angle of attack and therefore the lift, the value of K_l shall not normally exceed 2/3 according to Regulations.

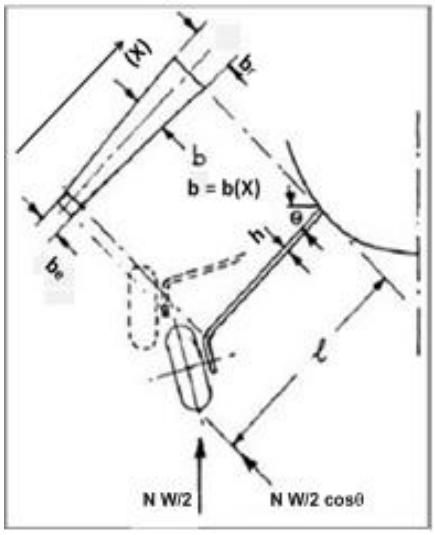

Figure 17 Leaf spring geometry gear

Other characteristics of the leaf spring that have to be considered are its material (there are examples of leaf spring made of steel, aluminum alloy or composite materials) and the shape of its section. Apart from the example of the box beam, adopted by Predators, the section of the leaf spring is normally rectangular with a "b" side (see Fig. 17) perpendicular to the deflection plane and the thickness, indicated by the letter h in Fig. 17. The section ratio, K_2, is given by:

$$K_2 = \frac{b}{h} \tag{4}$$

Figure 17 shows that usually b is not constant but it varies linearly with the leaf spring length, ranging from a maximum value b_R at the fixed end to b_E at the free end of the beam. The tapered beam has the advantage of reducing the mass of the beam itself towards the free end, where the bending stress also decreases. This implies a reduction of weight, even though the loads sustained are the same, and an increase of f and therefore of S and this is why this solution is frequently adopted (see Fig. 18).

Figure 18. example of tapered leaf spring landing gear

Once all inputs of the sizing activity have been defined, all various requirements may be expressed mathematically and then in a graph, which has S on the x-axis and h on the y-axis. S and h are the values that have to be determined:

Geometrical restriction on deflection shall be taken into account

(Requirement n° 1). Apart from the obvious capability of the leaf spring, considered as bend beam, of high deflection, the deflection of the landing gear cannot exceed a certain value, in order not to let the vehicle get too close to the ground, thus compromising the tail cone clearance (see Fig. 3). This constraint may by expressed as a function of ζ, i.e. the portion of vehicle's height (or landing gear's height) that is lost during compression:

$$S =< l \, sen \, \theta \, \varsigma \tag{5}$$

On the S-h graph (see Fig. 19) Requirement 1 is a vertical line that excludes all values of S that do not satisfy Eq. (5).

The vehicle's vertical energy at touchdown shall be absorbed (Requirement n° 2). The energy absorbed by the leaf spring is equal to half the product of maximum vertical deflection and corresponding maximum force of deflection. The energy that can be absorbed by the leaf spring has to be at least equal to the sum of the vertical kinetic energy of the vehicle at touchdown, of the work done, during deflection, by the weight W minus the work done, during deflection by the lift L.

$$\frac{1}{2} SNW >= \frac{1}{2} \frac{W}{9.81} V_z^2 + WS - LS \tag{6}$$

By introducing the ratio L/W and eliminating W, Eq. (6) may be rewritten as follows:

$$S >= \frac{\frac{V_z^2}{2 \cdot 9.81}}{0.5N - 1 - K_1} \tag{7}$$

On the S-h graph (see Fig. 19) Requirement 2 is a vertical line that excludes all values of S that do not satisfy Eq. (7). It is worth noting that Eq. (6) does not take into account the compression of the tire when loaded. This simplifying expression is however acceptable as the energy absorbed by the compression of the tire could be considered as an additional term for Eq. (7), which would make Requirement n° 2 less strict. However, it has to be remembered that, thanks to the energy absorbed by the tire, the vertical component of the leaf spring deflection would be a bit less than that of Eq. (7).

The beam shall be able to deflect (Requirement n° 3). The capability of deforming elastically of the leaf spring, thus making the required vertical deflection S possible, is related to the deflection f of the free end of the beam, as shown in Fig. 16. Remembering that the vertical deflection of the beam is given by Eq. (1) and that the bending moment acting on the beam is due to the application of the force $\frac{NW}{2} \cos\theta$ (component of the load perpendicular to the axis of the beam) to the free end of the beam, considering the expression of the deflection of the free end of the beam with a constant section:

$$f = \frac{4Ml^2}{Ebh^3} \tag{8}$$

where there is the elastic modulus of the material, E, and the moment of inertia of the rectangular section is expressed as follows:

$$I = \frac{bh^3}{12} \tag{9}$$

The deflection, f, can be expressed as follows:

$$f = \frac{S}{\cos\theta} = \frac{4N \frac{W}{2} \cos\theta l^3}{Ebh^3} \tag{10}$$

Introducing K_2 (see Eq. (4)) and expressing h, Eq. (10) becomes:

$$h^4 = \frac{4N\frac{W}{2}(\cos\theta)^2 l^3}{ESK_2} \tag{11}$$

Eventually Eq. (11) may be rewritten as:

$$h = \frac{K_3}{S^{0.25}} \tag{12}$$

Requirement n° 3 may be expressed on the S-h graph (see Fig. 19) by means of a slightly concave curve which decreases when S increases. This means that per each value of S there is an upper limit to the value of h. It is worth noting that Eq. (12) considers the section of the Leaf Spring constant, whereas the Leaf Spring is usually tapered, in order to better exploit the material with a reduction of weight and a higher deflection. Making the hypothesis, for sake of simplicity, of considering the Leaf Spring as a triangular tapered beam (referring to Fig. 17, you may make the hypothesis of considering the following variation of b: $b = b(X)$, specifically $b = (\frac{b_R}{l})X$, where b_R is given by $b_R = K_2 h$, according to Eq. (4)) and remembering that Eq. (8) derives from the integration of the increment of deflection along one finite element of the beam dX, df is given by:

$$df = \frac{MX}{EI} dX \tag{13}$$

Expressing the bending moment M as $M = PX$, the moment of inertia I according to Eq. (9) and b as a function of X, Eq. 13 may be rewritten as follows:

$$df = \frac{12PX^2}{E\frac{b_r}{l}Xh^3} dX \tag{14}$$

Integrating Eq. (14) we obtain:

$$f = \frac{6Ml^2}{Eb_r h^3} \tag{15}$$

By comparing Eq. (15) with Eq. (8), we understand that, if we consider all other parameters equal, the tapered Leaf Spring (with b=0 at the free end) increases its deflection by 50%. Eq. (10) and consequently Eq. (12) may therefore be multiplied by a so-called “Taper Factor”, T_f, which ranges between 1 (not tapered beam) and 1,5 (tapered beam with b=0 at the free end). This last case appears to be not so easily produced because of the practical need of connecting the wheel and the Leaf Spring. However, as shown in Fig. 19, reality is not that far from that extreme and taper factor equal to 1,3 may be acceptable. Eventually Requirement n°3 may be recalculated and a new curve in the S-h graph can be drawn.

The Leaf Spring shall be able not to deform plastically (Requirement n° 4). We consider the well known relationship of the maximum stress acting on the end of the beam opposite to the free one, where the bending moment has the highest value:

$$\sigma_{amm} = \left(6N\frac{W}{2}\cos\theta\, l\right)\left(b_r h^2\right) \tag{16}$$

By introducing K_2, Eq. (16) becomes:

$$\sigma_{amm} = \left(6N\frac{W}{2}\cos\theta\, l\right)\left(K_2 h^3\right) \tag{17}$$

Expressing h, we get:

$$h = K_4^{0.333} \tag{18}$$

Requirement n° 4 is represented through Eq. (18) on the S-h graph (see Fig. 19) and it is an horizontal straight line, which excludes the lower values of h.

The absorbed energy shall be damped (Requirement n° 5). This last requirement focuses on the lateral displacement of the wheel, which moves first toward the outside, during the leaf spring deflection, and then internally, when the leaf spring straightens itself. Thanks to the lateral displacement of the wheel that produces attrition with the ground, the leaf spring shall be able to damp the vehicle's vertical kinetic energy at touchdown. It is worth noting that the work done by the vertical deflection S and the weight W is absorbed during deflection and is returned part as the work done to make the weight move up to the height of the landing gear in static conditions and part as the residual potential energy of the CoG position in static conditions. The energy damped by the hysteresis of the tire during compression and successive extension is negligible. However taking into account this energy would just make the satisfaction of requirement n° 5 easier. In order to express mathematically this requirement, let us consider the two movements of the wheels first during compression and then during extension. In the first case the displacement is equal to S_0, as defined in Eq. (2), with a mean load acting on each single wheel given by the mean value between zero (at touchdown and therefore at the beginning of the movement of the wheel towards the outside) and $\frac{NW}{2}$ (when compression is complete). In the second case the movement is reduced because of the deflection in static conditions at the end of the extension. This movement may be evaluated, as first approximation, as $\frac{S_0(N-1)}{N}$, whereas the mean load is given by the mean value between $\frac{NW}{2}$ and $\frac{W}{2}$. By introducing the lateral friction coefficient of the tire K_{fl} and by considering both main landing gear elements, we get:

$$S\ W\ K_b\ K_{fl}\left(\frac{N}{2}+\frac{(N+1)}{2}\frac{(N-1)}{N}\right) >= \frac{1}{2}\frac{W}{9.81}V_z^2 \tag{19}$$

If we delete W, Eq. (19) may be rewritten as follows:

$$S >= \frac{\left(\frac{1}{2\ 9.81}V_z^{\ 2}\right)}{K_b\ K_{fl}\left(\frac{N}{2}+\frac{(N+1)}{2}\frac{(N-1)}{N}\right)} \tag{20}$$

In the S-h graph Requirement n°5 is therefore expressed by Eq. (20) as a vertical line, which tells us that S cannot be lower than the value given the member on the right hand side of Eq. (20). The constraint represented by Requirement n° 5 could become stricter (by introducing a coefficient in Eq. (20) a bit bigger than one), if we considered the compression of the tire, which would imply a reduction of the vertical deflection S of the leaf spring and therefore a reduction of S_0,

Figure 19 shows all five requirements on the S-h graph and highlights an area of compatibility, colored in grey in the figure. Figure 20 shows how design choices affect requirements, making them more or less severe for a design solution (S and h).

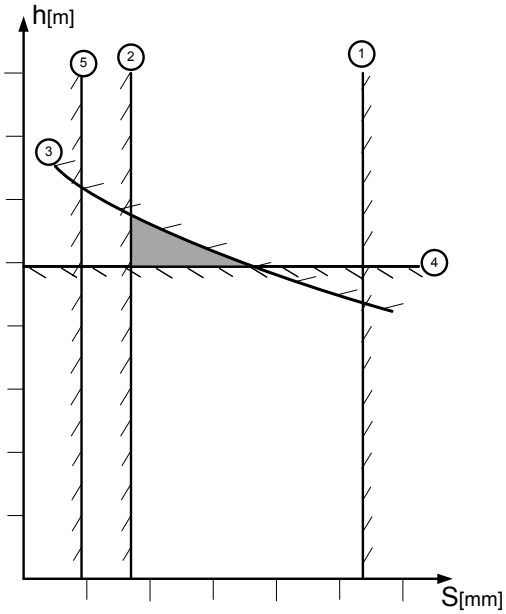

Figure 19. Graphical display of landing gear requirements

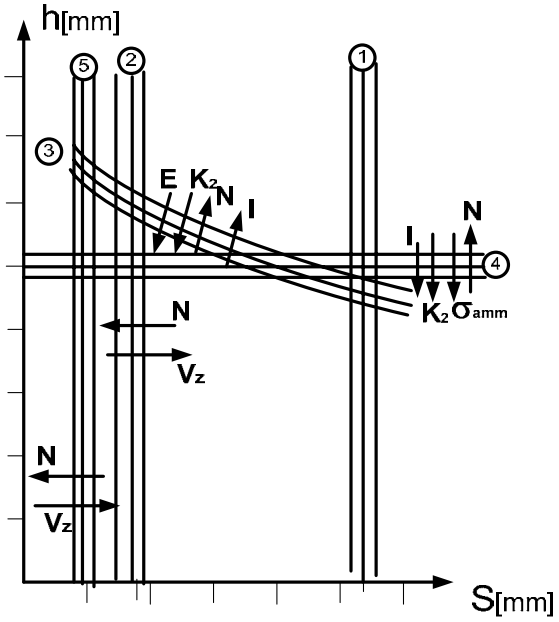

Figure 20. Influences of design parameters on requirements

V.Application of the Leaf Spring Landing Gear to a Space Reentry Vehicle

A. Leaf Spring landing gear sizing

Before starting any activity of landing gear sizing, it is absolutely necessary to define the reentry vehicle which will be equipped with landing gear. As the present paper aims at presenting a general methodology, not specifically applied to any reentry vehicles, we consider a hypothetical reentry vehicle (Reference Re-entry Vehicle, RRV) of such small size that the vehicle could be launched by VEGA launcher. Figure 21 shows RRV configuration, whereas Table 10 reports its main technical data.

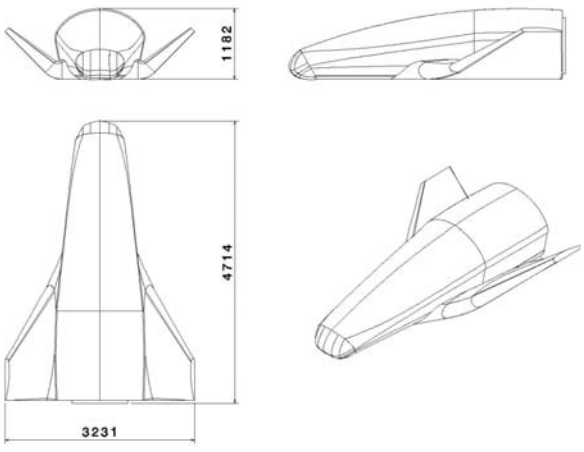

Figure 21. Reference Re-entry Vehicle configuration

Table 10. Reference Reentry Vehicle Technical Data

Length	4.5 m
High	1.2 m
Wingspan	3.2 m
Wing area	6.45 m^2
Mass	2000 kg
W/S	310 kg/m^2
Reference Launcher	VEGA

Among main design data of every flying vehicle, it is extremely important the capability of bearing the loads transmitted to the vehicle by the main landing gear elements at touchdown. As already mentioned and shown in Fig. 15 the main landing gear elements during landing transmit to the vehicle's structure a load equal to the product of the weight, sustained by the vehicle in static conditions, and N. Remembering that N is the number of "g" to define

the deceleration of the vehicle along the vertical axis and taking into account that the maximum value of N in Aeronautics ranges between 2.5 (civil transport aircraft) and 9 (fighters), in our case we may choose:

$$N = 3 \tag{21}$$

As far as the vertical velocity V_z is concerned, Airworthiness Regulations shall be applied (see Table 10, Ref. 5). Taking into account the RRV size and the fact that RRV is an unmanned vehicle, FAR 23 (General Aviation) may be considered as applicable regulations. Considering the minimum required value, we get:

$$V_z = 7 \text{ ft/s} = 2.13 \text{ m/s} \tag{22}$$

We can now proceed to make a hypothesis on the size of a main landing gear element of the same type as that shown in Fig. 16. Choosing l equal to 1200 mm and θ equal to 45°, we get a wheel track that is much better (for the probability of successful landing) than those of the other reentry vehicles in section III. Other assumptions are: K_l equal to 0.66, according to regulations; K_2, applied to the built in end section, equal to 6.6; the value of ζ is equal to 0.5 (percentage of compression which is acceptable with respect to the height of the vehicle); the characteristics of the material (we consider maraging steel[6,7] for the leaf spring), i.e. E, equal to 186000 N/mm^2; σ_{amm} equal to 1400 N/mm^2; all other technical characteristics of the RRV. Considering all these assumptions, the application of Eq. (5)-(7)-(12)-(18)-(20) is shown in Fig. 22.

As it can be seen in Fig. 22, there is an area of compatibility, on the basis of which we can choose, as design solution, h equal to 26 mm. In case of severe landing, with the maximum value for V_z (according to Eq. (23)) and consequently the maximum load factor N (according to Eq. (21)), all requirements will be met with adequate margin, except Requirement n° 4, which appears to be matched with limited margin, as usually happens in the aerospace field. In case of les severe landings, it is quite obvious that all requirements will be matched. Eventually it is worth noting that the small area of compatibility indicates compliancy of requirements.

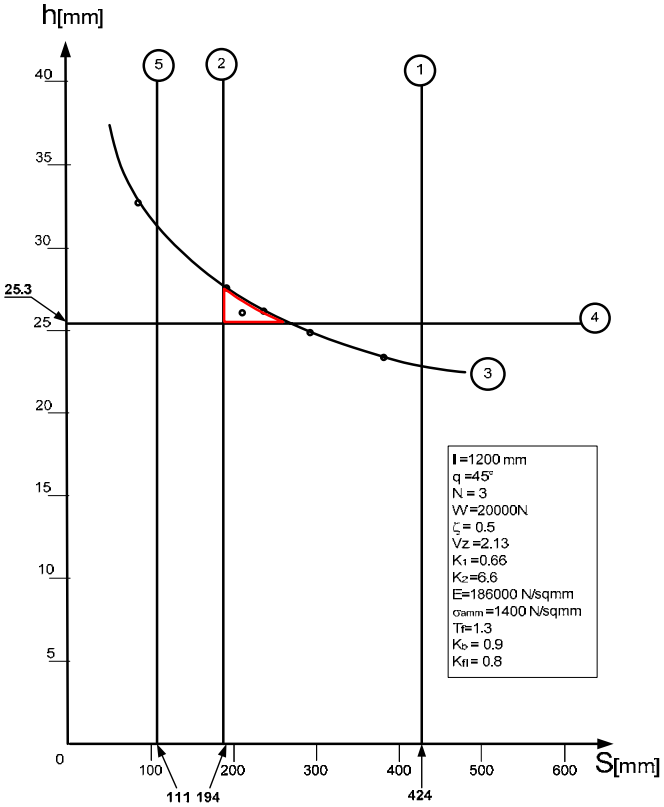

Figure 22. Sizing of leaf spring Landing Gear for RRV

B. FEM validation

In order to validate the results, the Leaf Spring has been evaluated through a FEM analysis, assuming h equal to 26 mm, V_z equal to 2.13 m/s and N equal to 3, for severe landings. The material considered for the leaf spring is maraging steel (Poisson module E=186000 N/mm^2 and σ_{amm}=1400 N/mm^2).

In order to perform FEM analyses, a 3D CAD model has been developed as the basis for the FEM model. Figure 23 shows the reference geometry. The leaf spring consists of a tapered plate of constant thickness (h=26 mm), with the longest side equal to 171.6 mm and the shortest side equal to 60 mm. The length of the longest side is defined by the ratio of the thickness h and the longest side itself ($K_2 = \frac{b_r}{h} = 6.6$). The FEM model has been developed with a linear Octree tetraedric mesh with a global size of 20 mm. Figure 24 shows the mesh of the leaf spring, the constraint condition and the load condition. The leaf spring is built in beam. The load condition corresponds to a distributed force applied to the thickness of the minor base of the beam with total magnitude equal to 29430 N.

Figure 25 and Fig. 26 show the results of the FEM analysis. The vertical displacement at the free end of the Leaf Spring is equal to 215 mm, whereas from Fig. 22 and Requirement n° 3 we get a deflection equal to 240 mm, which is about 10% higher than the value obtained by FEM analysis and therefore still acceptable. The highest stress in the built in end section is 1338 N/mm^2, which is lower than the value of σ_{amm} (yield stress) of the chosen material. Once that the FEM analysis is over and the leaf spring adequately matches requirements, it is important to evaluate its mass, which, starting from the volume equal to 3600 cm^3 and considering the specific weight of the steel equal to 7.8 g/cm^3, is equal to 28.1 kg per each leaf spring.

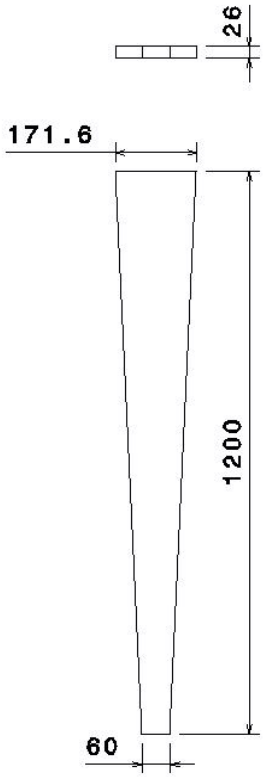

Figure 23. Leaf spring geometry

Figure 24 FEM mesh model

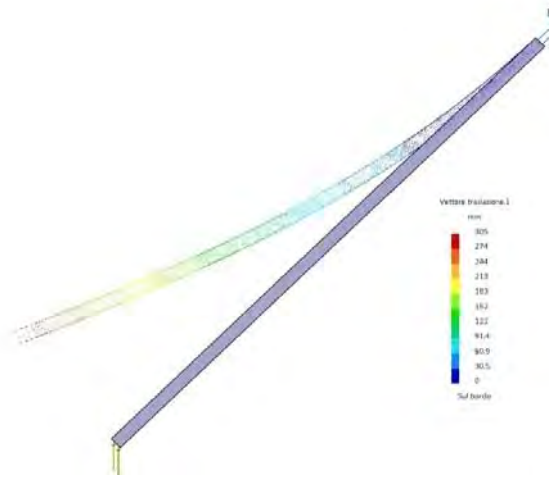

Figure 25. FEM analysis result - displacements

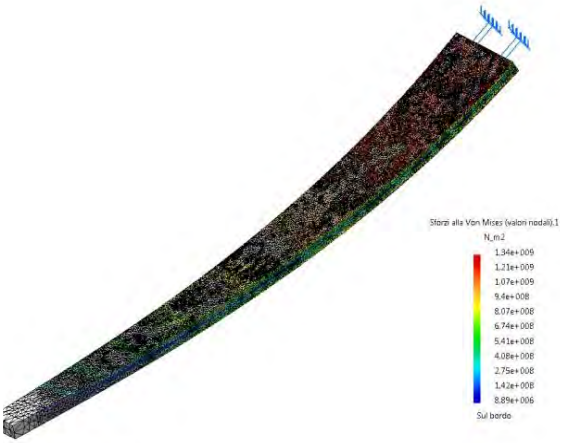

Figure 26. FEM analysis result - stress

C. Nose Landing Gear

The Main Landing Gear is without any doubts the most important part of the entire landing gear system and for this reason we have focused our attention on it, also because the adoption of the Leaf Spring landing gear for a reentry vehicle is quite unusual. However, for sake of completeness, in this sub-section we also deal briefly with the Nose Landing Gear. First of all it is worth noting that the Leaf Spring cannot be adopted for the Nose Landing Gear, as the lateral displacement of the tire cannot be used to damp the energy absorbed during the impact of the wheel with the ground. In fact, the Nose Landing Gear, besides guaranteeing stability and maneuvering of the vehicle when it is moving on ground, works also during landing and during the successive deceleration phase. The loads acting on the Nose Landing Gear during these two phases are useful to size the landing gear itself. In fact, even if the correct landing envisages that the vehicle's vertical kinetic energy is absorbed and damped only by the main landing gear, it may happen that part of the vehicle's vertical kinetic energy could be absorbed by the nose landing gear. This situation may occur for instance during landing (in case the landing maneuver is not correctly performed) when the nose landing gear touches the ground before the main landing gear has absorbed all vehicle's vertical kinetic energy. The so-called level landing, defined by Airworthiness Regulations as the landing maneuver when the main landing gear and the nose landing gear touch the ground simultaneously, is the operative scenario considered for the nose landing gear sizing. In this case, referring to Fig. 15 and considering the weight W multiplied by the load factor N, the force acting on the nose landing gear is given by:

$$R_{NLDG} = \frac{NWm}{L} \tag{23}$$

Considering the RRV and its values, Eq. (23) becomes:

$$R_{NLDG} = \frac{3 \cdot 20000 \cdot 0.264}{2.64} = 6000\ [N] \tag{24}$$

Referring to Fig. 27, in case of deceleration after touchdown, considering the force generated by the brakes of main landing gear's wheels and applied to the wheels where there is contact with ground, we have a deceleration $\ddot{X}$ and therefore a force of inertia given by:

$$-m\ddot{X} = F_{breaking} \tag{25}$$

Referring to Fig. 27, the equation of the moment with respect to contact point between ground and the wheels of the main landing gear, we get to the relationship which expresses the load acting on the Nose Landing Gear (that has to be summed to the static load):

$$\Delta R_{NLDG} = \frac{W\ddot{X}H}{gL} \tag{26}$$

Introducing the values of RRV and assuming a maximum deceleration during breaking equal to 5 m/s^2, Eq. (26) becomes:

$$R_{NLDG} = \frac{2000 \cdot 5 \cdot 1.4}{2.64} = 5300\,[N] \tag{27}$$

which has the same order of magnitude of Eq. (25), but, unlike Eq. (25), this load always occurs whenever the vehicle lands. As the value assumed for the deceleration is not high, a drag chute able to generate a much higher deceleration may be adopted, as in case of the X 37. The drag chute may be a good solution also because it would not overload the Nose Landing Gear, as the force that it generates is applied to the vehicle's CoG and not to the ground. In case the drag chute is installed on board the vehicle, the wheels of the Main Landing Gear are anyway equipped with brakes that can be used at low speed, when the drag chute is not operative anymore. In order to absorb these loads and thus to damp the related energy, as already mentioned, the Nose Landing Gear cannot be a Leaf Spring. However, aiming at avoiding fluidic systems and pursuing simple, and therefore reliable and affordable, solutions, also for the Nose Landing Gear we have considered the use of a "rubber spring shock absorber". This system consists of rubber disks, which compress elastically to absorb the energy and then, thanks to the hysteresis of the rubber, damp it, are relatively common for light aircraft (see Fig. 28). Their shock absorber efficiency is a little bit higher than that of metallic spring (efficiency=0,6), but, unlike other systems like air or oleo/pneumatic spring, rubber spring shock absorbers do not have any sealing problems and are therefore highly reliable. As an alternative, particularly to avoid problems that may arise for rubber disks because of the space environment, we believe that a promising solution may be the use of systems with nest spring generating internal dry friction. Against the disadvantage of having a damping not proportional to the speed of compression/extension of the shock absorber, these systems are very simple and reliable and were largely used in the past in the automotive field as well as in the aeronautical field, where there were few significant applications, like the shock absorber "Kronprinz" of the Ju 87 "Stuka" vehicle (made of aligned metallic rings, which, deforming under compression, generate friction and therefore dissipation of energy, see Fig. 29)).

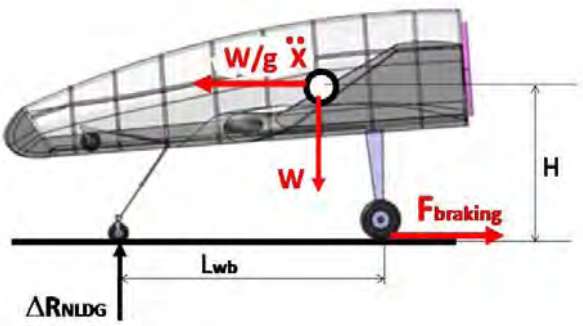

Figure 27. Deceleration load on Nose Landing Gear

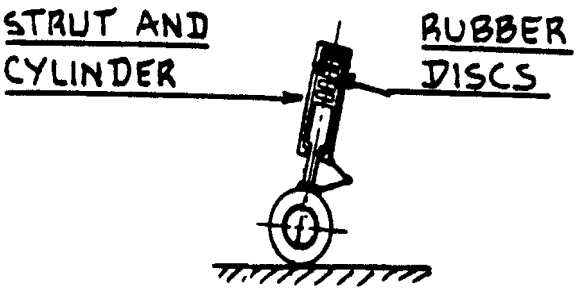

Figure 28. Rubber discs shock absorber (Ref. 3)

Figure 29. Dry friction shock absorber (Ref. 8)

D. Landing Gear Integration with the Vehicle

In order to complete the study, we have performed an activity of system integration of the proposed landing gear with the hypothesized Reference Reentry Vehicle (RRV). The Leaf Spring Main Landing Gear is stowed in a very small cavity when retracted. This is the smallest cavity that we can have, considering all various types of landing gear. As Fig. 30 shows, the retracted landing gear is stowed into a cavity exactly equal to the metallic plate, where there is the leaf spring, and into another cavity exactly equal to the volume of the wheel, where there is the wheel itself. The landing gear, when retracted, has the least effect on the airframe structure, as there is no need to create great cavity into the vehicle's primary structure. In order to have the retracted landing gear configuration, shown in Fig. 30, the kinematics of the landing gear extension has to be equipped with hinges, which allow the wheel to be correctly positioned and the leaf spring to rotate at least along two planes. It is worth remembering that, as this type of vehicles does not take-off in a traditional way but it is lifted off by a launcher vehicle, the kinematics of the landing gear extension does not have to be able to retract the landing gear. Therefore the kinematics for the landing gear extension may be activated by a system of springs that allow the extended landing gear to be located and blocked into a definitive position. Moreover it has to be considered the favorable effect for the landing gear extension of the aerodynamic and gravity forces, which generate torques that help the landing gear extension.

Also for the Nose Landing Gear the aerodynamic forces favorably contribute to its extension, thanks to the type of mechanism that has been chosen. The same considerations made for the Main Landing Gear elements still apply. There are springs that make the system move. These springs allow the leg of the Nose Landing Gear to be opened and the wheel to be correctly positioned (when stowed in the fuselage, the wheel is rotated in order to reduce the necessary cavity, see Fig. 30). If the wheel of the Nose Landing Gear had been stowed parallel to the bottom surface of the fuselage, the cavity of the retracted landing gear would have been smaller. However this solution has been discarded, as a failure of the mechanism for the correct wheel positioning is critical for landing. The chosen configuration guarantees a successful landing, even if, in case of failure, the wheel mechanism is jammed.

Figure 30 shows the main structural layout of the fuselage. It consists of frames connected by longitudinal stringers, which give the airframe the necessary stiffness. The main landing gear is attached to one spar frame, where is also attached one main wing spar. Also the Nose Landing Gear is attached to one fuselage bulkhead. Bulkheads are also shaped in such a way to allow the integration of the landing gear inside the fuselage. It is worth noting that the retracted configuration of the landing gear has the leas effect on the airframe structure, if we consider an original design of the vehicle without landing gears[9,10]. The wheels of the Main Landing Gear are stowed into a cavity between two bulkheads, in order not to affect badly the vehicle's structural configuration.

As far as the weight of the landing gear is concerned, a good estimation is possible also if a detailed design has not be performed. In particular the weight estimation of the leaf spring is possible with good approximation considering that the analytical design has been confirmed by the numerical FEM analysis. The weight of the leaf spring is 2 x 28 kg to which the weight of the wheels (7-8 kg) and of the deploying mechanism (10 kg) must be added. Thus, the total weight of the main landing gear results 74 kg. Considering that, usually, the weight of the nose landing gear results about the 20 - 25 % of the total weight, a good estimation of the nose landing gear weight is 100 kg. This is the 2 % of the total aircraft weight, thus fully plausible[11-14].

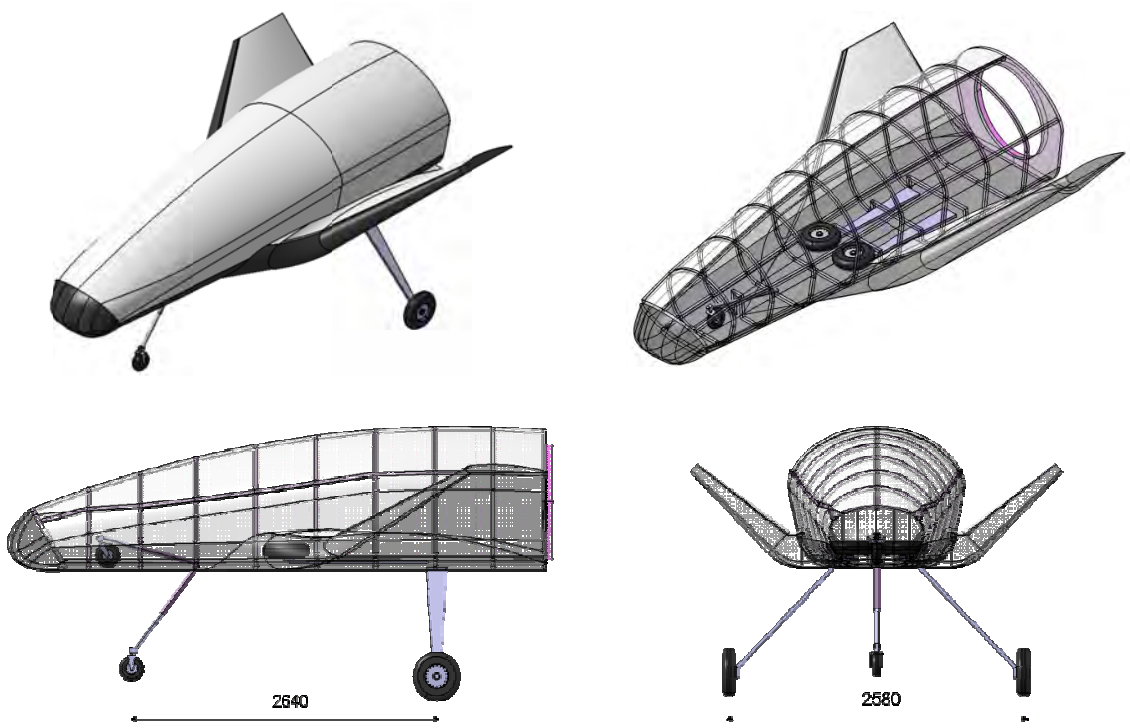

Figure 30 Landing Gear integration with the vehicle

VI.Conclusion

The estimation of the weight of the landing gear for RRV is coherent with the state of the art of aerospace technology, notwithstanding the unusual innovative solution. We believe that this study proves the feasibility of the proposed solution and we think that more detailed analyses are worthwhile. The proposed solution appears to be simple and therefore reliable and affordable. Moreover it seems to have the least effect on the design of the remaining parts of the vehicle, the least effect in terms of limited required cavity to stow the landing gear elements when retracted and of limited constraints on the optimal shape of the vehicle's structure to match requirements. Taking into account all advantages that can come from the adoption for a technology demonstrator of a reentry vehicle of the landing gear, we do hope that we have contributed to reach the goal.

Acknowledgments

The authors wish to thank Federico Massobrio of Thales Alenia Space-Italy for the fruitful exchange of ideas and interesting scientific discussions.

References

[1]Chiesa S., Camatti D., Corpino S., Pasquino M., Viola N., "Affordable Technological Demonstrator for Hypersonic Flight," *4th International Seminar on RRDPAE*, Warsaw, Dec. 2000.

[2]Chiesa S., Grassi M., Russo G., Teofilatto P. "A Small-Scale Low-Cost Technology Demonstrator of a Reusable Launch Vehicle," *13th AIAA/CIRA International Space Planes and Hypersonic Systems and Technologies Conference*, 16-20 May 2005.

[3]Currey, N. S., *Aircraft Landing Gear Design: Principles and Practices*, AIAA Education Series, 2nd ed., AIAA Inc., Washington, DC, 1988, Chaps 5.5. p 85.

[4]Pazmany L., *Landing Gear Design for Light Aircraft Vol.1*, Pazmany Aircraft Corporation, San Diego, 1986, Chap 10 p 152.

[5]Roskam, J., *Airplane Design - Part 4: Layout Design Of Landing Gear And Systems*, 2nd ed., Design Analysis & Research Co., Ottawa, 1989.

[6]Rohrbach, K, Schmidt, M., *Properties and Selection: Irons, Steels, and High-Performance Alloys*, ASM Handbook, Vol. 1, 10th ed.. ASM International, Ohio, 1993.

[7]Cardile, D., Viola, N., Chiesa, S., Rougier, A., "Applied Design Methodology for Lunar Rover Elastic Wheel," *Acta Astronautica* 81, 2012, pp. 1-11.

[8]Gabrielli, G., *Lezioni Sulla Scienza Del Progetto Degli Aeromobili*, Vol. II, Ed. Levrotto & Bella, Torino, 1975.

[9]Carrera, E., Chiesa, S., Corpino, S., "Manufacturing and Economic Constraints on the Structural Design of a Reduced-Sized Technological Demonstrator," *24th ICAS Congress*, Yokohama, Aug.-Sept. 2004.

[10]Chiesa, S., Carrera, E., Corpino, S., Triffiletti, S., Russo, G., Curreri, F., "Comparison of Various Structural Solutions for a Reduced-Sized Technological Demonstrator," *13th AIAA/CIRA International Space Planes And Hypersonic Systems And Technologies Conference*, May 2005.

[11]Chiesa, S., Maggiore, P., "Hypersonic Aircraft Conceptual Design Methodology," *19th Congress Of ICAS*, Anaheim, California, Sept. 1994.

[12]Antona, E., Chiesa, S., Corpino, S., Viola, N., "L'Avamprogetto dei Velivoli," *Atti Dell'accademia Delle Scienze Di Torino*, Torino, 2009.

[13]Chiesa, S., Viola, N., "Sub-Systems Equipments Weight and Volume First Estimation, a Tool for Aircraft Conceptual Design," *International Journal Of Mechanics and Control*, Vol. 08, No 01, Jul 2007.

[14]Chiesa, S., Fioriti, M., Viola, N., *Methodology For An Integrated Definition Of A System And Its Subsystems: The Case-Study Of An Airplane And Its Subsystems*, Systems Engineering - Practice And Theory, Intech, 2012.